Defective insulin receptor activation and altered lipid rafts in Niemann–Pick type C disease hepatocytes

Saara VAINIO*†, Igor BYKOV*, Martin HERMANSSON‡, Eija JOKITALO†, Pentti SOMERHARJU‡ and Elina IKONEN†‡[1]

*National Public Health Institute, Helsinki, Finland, †Institute of Biotechnology, University of Helsinki, Haartmaninkatu 8, FIN-00014, Finland, and ‡Institute of Biomedicine, University of Helsinki, Haartmaninkatu 8, FIN-00014, Finland

Niemann–Pick type C (NPC) disease is a neuro-visceral cholesterol storage disorder caused by mutations in the *NPC-1* or *NPC-2* gene. In the present paper, we studied IR (insulin receptor) activation and the plasma-membrane lipid assembly in primary hepatocytes from control and NPC1–/– mice. We have previously reported that, in hepatocytes, IR activation is dependent on cholesterol–sphingolipid rafts [Vainio, Heino, Mansson, Fredman, Kuismanen, Vaarala and Ikonen (2002) EMBO Rep. **3**, 95–100]. We found that, in NPC hepatocytes, IR levels were up-regulated and the receptor activation was compromised. Defective IR activation was reproduced in isolated NPC plasma-membrane preparations, which displayed an increased cholesterol content and saturation of major phospholipids. The NPC plasma membranes were less fluid than control membranes as indicated by increased DPH (1,6-diphenyl-1,3,5-hexatriene) fluorescence anisotropy values. Both in NPC hepatocytes and plasma-membrane fractions, the association of IR with low-density DRMs (detergent-resistant membranes) was increased. Moreover, the detergent resistance of both cholesterol and phosphatidylcholine were increased in NPC membranes. Finally, cholesterol removal inhibited IR activation in control membranes but restored IR activation in NPC membranes. Taken together, the results reveal a lipid imbalance in the NPC hepatocyte, which increases lipid ordering in the plasma membrane, alters the properties of lipid rafts and interferes with the function of a raft-associated plasma-membrane receptor. Such a mechanism may participate in the pathogenesis of NPC disease and contribute to insulin resistance in other disorders of lipid metabolism.

Key words: cholesterol, insulin, lipid raft, liver, Niemann–Pick type C, sphingolipidosis.

INTRODUCTION

Niemann–Pick type C (NPC) disease is an autosomal, recessively inherited lysosomal storage disorder, characterized by endo-lysosomal accumulation of unesterified cholesterol and sphingolipids [1]. The disease is caused by mutations in the *NPC-1* or *NPC-2* gene but the exact functions of the encoded proteins remain elusive. Although NPC disease is often considered to be a primary cholesterol trafficking disorder, defects in the transport of sphingolipids and fatty acids have also been proposed as the underlying cause [1,2]. Lipid accumulation occurs in most, if not all, cells of NPC patients; however, typically for storage diseases, the liver is one of the most lipid-laden tissues [3]. Originally, accretion of cholesterol in NPC cells was considered to derive from endocytosed LDLs (low-density lipoproteins) but it has been shown that other pools, such as endogenously synthesized cholesterol, may contribute to the storage [4]. It is generally acknowledged that the endosomal cholesterol sequestration is coupled with impaired cholesterol transport to other cellular destinations, such as the plasma membrane and ER (endoplasmic reticulum). However, controversial data regarding the amount of cholesterol in the plasma membrane of NPC cells have been reported (reviewed e.g. in [1]).

Cholesterol- and sphingolipid-rich membrane microdomains, termed lipid rafts, have been implicated in the regulation of various cellular processes, including membrane trafficking and cell signalling [5,6]. Many key signalling molecules have been shown to function via lipid rafts, and one such molecule is the IR (insulin receptor) [7,8]. Its ligand, the anabolic hormone insulin, has a central role in controlling both glucose and lipid metabolism at the whole-body level and is also indispensable for the growth and well-being of many cell types [9]. IR belongs to the family of receptor tyrosine kinases and, upon insulin binding, it undergoes a conformational change and autophosphorylation on tyrosine residues on intracellular β-subunits [10]. This in turn initiates a cascade of tyrosine phosphorylations of downstream targets [11]. The role of lipid rafts in IR signalling has been studied in several insulin target cells. In adipocytes, the role of caveolae and caveolin-1 in IR function and especially in the assembly of the downstream signalling cascade has been demonstrated (reviewed in [8]). In pancreatic β-cells, the two isoforms of IR have been shown to be differentially regulated via lipid rafts [12]. We have previously shown that, in hepatocytes, the active form of IR is recruited to lipid rafts, and treatments affecting this recruitment also affect IR activity [13]. These results suggest that the optimal function of IR is dependent on the lipid environment.

In the present paper, we studied the function of IR and plasma-membrane lipid composition in primary hepatocytes from control [WT (wild-type)] and NPC1–/– (NPC) mice. In the mouse, a naturally occurring mutation in NPC1 leads to a phenotype closely resembling the human disease [14]. It has earlier been proposed that cholesterol–sphingolipid rafts accumulate in the late endosomal compartments of NPC cells, potentially contributing to the disease pathogenesis [15,16]. The present findings suggest that the NPC1 defect also leads to perturbations in plasma-membrane rafts and raft-dependent signalling. We provide evidence that, in NPC hepatocytes, the activation of IR is compromised and the composition and ordering of plasma-membrane lipids differ

Abbreviations used: DPH, 1,6-diphenyl-1,3,5-hexatriene; DRM, detergent-resistant membrane; ER, endoplasmic reticulum; HDL, high-density lipoprotein; IR, insulin receptor; LDL, low-density lipoprotein; NPC, Niemann–Pick type C; PC, phosphatidylcholine; PL, phospholipid; pTyr, phosphorylated tyrosine residue; SM, sphingomyelin; WT, wild-type.

[1] To whom correspondence should be addressed (email elina.ikonen@helsinki.fi).

from normal. These differences are accompanied by altered characteristics of plasma-membrane lipid rafts, which in turn may account for the defect in IR function.

EXPERIMENTAL

Hepatocyte isolation and cell culture

Control and NPC1–/– (NPC) Balb/c mice were maintained and identified as described in [17] following the guidelines of the National Public Health Institute, Finland, for the use and care of laboratory animals. Primary hepatocytes from 7-week-old mice were isolated by the collagen-perfusion method as described in [18,19] and maintained in Eagle's minimal essential medium supplemented with 10 % (v/v) foetal bovine serum, 10 mM Hepes, 100 units/ml penicillin and 100 μg/ml streptomycin. After isolation, the viability of the cells was determined by Trypan Blue (Sigma) staining. The cells were always used within 24 h of isolation. Huh7 cells were cultured as described in [20]. Cell-culture reagents were from Gibco BRL (Basel, Switzerland).

Insulin stimulation

Cells were serum-starved for 2–4 h before insulin stimulation, which was performed in serum-free medium supplemented with 100 nM insulin (Actrapid®; Novo-Nordisk, Bagsværd, Denmark). Thereafter, cells were washed with ice-cold PBS and lysed in 1 % SDS in 10 mM Tris/HCl (pH 7.4). The washing and lysis buffers contained phosphatase inhibitors (1 mM each of Na_3VO_4, NaF and okadaic acid; Sigma) and protease inhibitors (25 μg/ml each of chymotrypsin, leupeptin, antipain and pepstatin A; Sigma).

Western blotting

Western blotting was performed essentially as described in [13]. Protein concentrations were determined using a Bio-Rad DC Protein Assay kit. Cellular protein (20 μg or equal volumes from gradient fractions) was used for experiments unless otherwise indicated. For blocking the filters, 5 % dried milk [for anti-IRβ; rabbit polyclonal (Transduction Laboratories, Lexington, KY, U.S.A.) for anti-calnexin; rabbit polyclonal (kindly provided by Dr A. Helenius, Institut für Biochemie, ETH-Hönggerberg, Zurich, Switzerland) for anti-Na^+/K^+-ATPase; clone α6F for anti-LAMP1; clone 1D4B (Developmental Studies Hybridoma Bank, University of Iowa, U.S.A.)] or 3 % BSA [for anti-pTyr (phosphorylated tyrosine residue); clone 4G10 (Upstate Biotechnology, Lake Placid, NY, U.S.A.)] was used. For analysis of IR activity, filters were probed with anti-pTyr antibody, stripped with 1 M glycine (pH 3.1), washed, reblocked and reprobed with anti-IRβ antibody. The signal from horseradish-peroxidase-conjugated secondary antibodies was visualized by enhanced chemiluminiscence detection (ECL® Western blotting detection kit, Amersham Biosciences) on X-ray films and several exposure times were taken to ensure the linearity of signal intensity. Quantification of Western blotting results was performed as described in [13] by determining the band intensities using the Phospho-Imager Tina 2.1 software (Raytest Isotopenmessgeraet GmbH, Straubenhardt, Germany). Activation of IR was determined as the ratio of anti-pTyr and anti-IRβ band intensities in the same blot.

Isolation of plasma-membrane fractions

Livers from 7-week-old WT and NPC mice were homogenized using a Dounce homogenizer and a syringe and 22G-needle and then centrifuged for 15 min at 16000 ***g*** at 4 °C. The supernatant was adjusted to 1.7 M sucrose (16 ml) and overlaid with 1.2 M (16 ml) and 0.8 M (7 ml) sucrose in 10 mM Hepes, 2 mM EGTA and 1 mM dithiothreitol. Centrifugation (25000 rev./min for 24 h at 4 °C) was performed with a Beckman SW-28 rotor (gradient 1). The 0.8/1.2 M interphase was collected, adjusted to 0.8 M sucrose (4 ml) and overlaid with 0.5 M (4 ml)/0.3 M (2 ml)/0.2 M (2 ml) sucrose and centrifuged in an SW-40 rotor for 16 h at 30000 rev./min at 4 °C (gradient 2). The 0.5 M/0.8 M interphase was collected and recovered on a 2.4 M sucrose cushion by centrifuging at 20000 rev./min for 1.5 h at 4 °C. The samples were then dialysed against 10 mM Hepes and 10 mM NaCl (kinase buffer).

IR kinase assay

Protein (20 μg/sample) from plasma-membrane preparations was used. $MgCl_2$ and $MnCl_2$ were added to a final concentration of 5 mM and the volume was adjusted to 20 μl with kinase buffer. Insulin (10 nM) was added and the samples placed on a shaking (7 ***g***) water bath at 37 °C. After 5 min, 1 mM ATP (Sigma) was added and the incubation continued for 5–15 min. The reaction was terminated by adding 0.25 M EDTA, 10 mM Na_3VO_4 and SDS-loading buffer. Samples were analysed by Western blotting. For studying the effect of phosphatase inhibitors and methyl-β-cyclodextrin, the samples were first incubated in the presence of 1 mM Na_3VO_4, NaF and ocadaic acid or 10 mM methyl-β-cyclodextrin (Sigma) for 30 min at 37 °C with shaking and then processed as above.

Analysis of DRMs (detergent-resistant membranes)

Optiprep density-gradient fractionation in the presence of 1 % Triton X-100 was used for DRM isolation as described in [13,21]. For plasma-membrane fractions, 50–100 μg of total protein was used as starting material. For analysing the amount of ^{125}I-insulin in DRMs, cells were treated with 200 pM ^{125}I-insulin (specific radioactivity 2000 Ci/mmol, Amersham Biosciences) for 5 min, washed extensively and subjected to gradient fractionation. Radioactivity was measured with a Wallac 1470 Automatic Gamma counter. Unspecific binding, measured by performing the experiment in the presence of 100 nM unlabelled insulin, was subtracted from the values. For analysing lipid solubility, cells were labelled with 900 nM (1 μl/ml) [^{14}C]cholesterol or 3 nM (1 μl/ml) [^{3}H]choline chloride (specific radioactivities 58.0 mCi/mmol and 80.0 Ci/mmol respectively, Amersham Biosciences) for 24 h before fractionation. For [^{14}C]cholesterol, radioactivity was directly measured with a Wallac Winspectral 1414 liquid-scintillation counter. For [^{3}H]PC (where PC stands for phosphatidylcholine) and [^{3}H]SM (where SM stands for sphingomyelin), lipids were extracted by methanol/chloroform and PC and SM were separated by TLC as described in [21].

Analysis of lipid composition

Samples for MS were processed and analysis was performed with a Quattro Micro triple quadrupole mass spectrometer (Micromass Limited, Altrincham, Cheshire, U.K.) essentially as described in [22]. For determining cholesterol levels, lipids were extracted with methanol/chloroform and total and free cholesterol determined using a Chol R1 kit (Roche, Indianapolis, IN, U.S.A.) or a free cholesterol C kit (Wako Chemicals, Osaka, Japan). Total phosphate was determined as described in [23].

Determination of membrane fluidity

The 'fluidity' of purified plasma membranes was determined by measuring the steady-state anisotropy of DPH (1,6-diphenyl-1,3,5-hexatriene) essentially as described in [24]. Briefly, DPH

(5 mM) in tetrahydrofurane was injected into Tris/HCl (0.1 M) buffer (20 μM final concentration) followed by vigorous vortex-mixing for 1 min. Aliquots of this DPH solution were then added to a microcuvette (4 mm light path) containing plasma membranes [60 nmol of PL (phospholipid)] dispersed in the same buffer to achieve a DPH/PL ratio of 1/100. After vortex-mixing, the sample was incubated at 37 °C for 25 min before measurements on a Varian Cary Eclipse fluorescence spectrophotometer equipped with a thermostatted cuvette holder set to 37 °C. The excitation and emission wavelengths were 362 and 426 nm respectively.

Other methods

For electron microscopy, samples from 0.8/1.2 M (gradient 1) and 0.5/0.8 M (gradient 2) interphases were fixed with 0.2 % glutaraldehyde (EM-grade; Electron Microscopy Sciences, Hatfield, PA, U.S.A.)/2 % (w/v) paraformaldehyde in 100 mM Na_2HPO_4 buffer for 30 min at room temperature (23 °C) and collected by centrifugation (16000 ***g*** for 30 min at 4 °C). The pellets were post-fixed for 1 h at room temperature with 1 % osmium tetroxide and 1.5 % cyanoferrate in 0.1 M sodium cacodylate buffer (pH 7.4), dehydrated and embedded in Epon 812 (TAAB Laboratories Equipment, Aldermaston, Berks., U.K.). Then, 60–70 nm thick sections were cut and post-stained with uranyl acetate and lead citrate and then examined with an FEI Tecnai 12 transmission electron microscope at 80 kV. Immunofluorescence and filipin stainings were performed as described in [25], except that acetone fixation (5 min at − 20 °C) was used for anti-IRβ and anti-LAMP1 antibodies. Fluorescently labelled secondary antibodies (goat anti-rabbit, Alexa Fluor® 488; and rat anti-mouse, Alexa Fluor® 568) were obtained from Molecular Probes. Before fixing, the cells were serum-starved for 2 h and then left untreated or stimulated with insulin for 1–60 min. Images were captured with an Olympus IX71 inverted microscope (filipin staining) or with a Leica TCS SP2 AOBS confocal microscope (anti-IRβ and anti-LAMP1 stainings).

RESULTS

IR localization in WT and NPC hepatocytes

Primary hepatocytes were isolated from 7-week-old WT and NPC Balb/c mice using the collagen-perfusion method, and the cells were used within 24 h of isolation. Both WT and NPC cells were viable and attached well on gelatin-coated cell-culture dishes. NPC hepatocytes exhibited the characteristic perinuclear depositions of free cholesterol, as revealed by filipin staining (Figure 1A). To analyse the subcellular distribution of IR, we performed immunofluorescence staining of cells cultured in the absence of insulin. Anti-IRβ antibodies revealed a punctuate plasma-membrane staining pattern in both WT and NPC cells, with no co-localization with the late endosomal/lysosomal marker LAMP1 (Figure 1B). This pattern is consistent with the reported uneven distribution of IR in the hepatocyte plasma membrane, with most of the receptors concentrated in microvilli [26]. In NPC cells, the anti-LAMP1 antibody staining pattern was typically more centrally clustered than in WT cells, reflecting the characteristic distribution of the storage lysosomes [27]. The staining pattern of IR and LAMP1 was also studied after various times of insulin stimulation (1–60 min). The two markers exhibited clearly distinct distribution at all the time points analysed (results not shown).

IR expression and activation in WT and NPC hepatocytes

To study the expression levels and activation of IR, isolated hepatocytes were stimulated with insulin (or left untreated) and analysed by Western blotting. The total amount of IR was detected with anti-IRβ antibodies and the activated receptor was visualized with an antibody raised against pTyr. We found that the levels of IR in NPC hepatocytes were up-regulated approx. 50 % in comparison with WT cells (Figures 2A and 2B). This up-regulation was detected in all the mice analysed and was not caused by the *in vitro* incubation, since it was also seen in liver lysates from NPC mice (results not shown). Despite the higher receptor levels, the amount of activated IR did not differ between WT and NPC cells, revealing a defect in the relative activation efficiency of NPC-IR (Figure 2A). This defect was observed at several time points of insulin stimulation (Figure 2C). As the NPC-IR was localized to the plasma membrane and not sequestered to a compartment inaccessible to insulin, it was conceivable that the higher amount of IR was needed to compensate for the poor activation of the receptor.

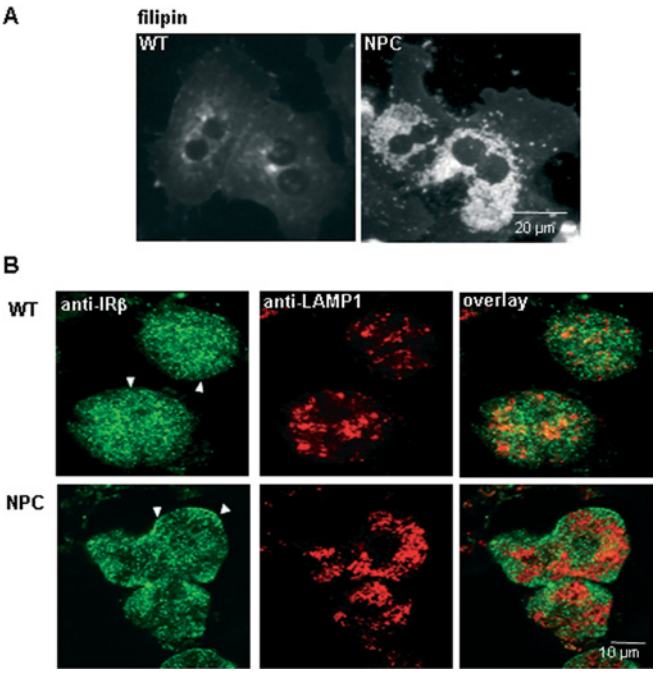

Figure 1 Fluorescent images of WT and NPC hepatocytes

(**A**) Primary hepatocytes from WT and NPC mice were grown on coverslips, fixed with paraformaldehyde and stained with filipin to visualize the distribution of unesterified cholesterol. In NPC cells, the perinuclear cholesterol storage organelles are clearly visible. (**B**) Serum-starved WT and NPC hepatocytes were fixed with acetone and stained with anti-IRβ and anti-LAMP1 antibodies followed by Alexa Fluor® 488- and Alexa Fluor® 568-conjugated secondary antibodies respectively. Confocal images were captured at the cell-surface level to illustrate the plasma membrane staining of IR (arrowheads). The majority of LAMP1-positive organelles are out of this focal plane.

Plasma-membrane isolation

IR autophosphorylation occurs rapidly after insulin binding, which takes place at the plasma membrane. As the activation defect in NPC cells was observed within the first minutes of insulin stimulation (Figure 2C), we hypothesized that the underlying cause might be at the level of the plasma membrane. We therefore isolated plasma-membrane fractions from WT and NPC mouse livers by sequential gradient fractionation. The depletion of contaminating membranes and enrichment of plasma-membrane markers were analysed by Western blotting and the ultrastructure of the preparations by electron microscopy. After gradient 1, contaminating membranes were still abundant, since

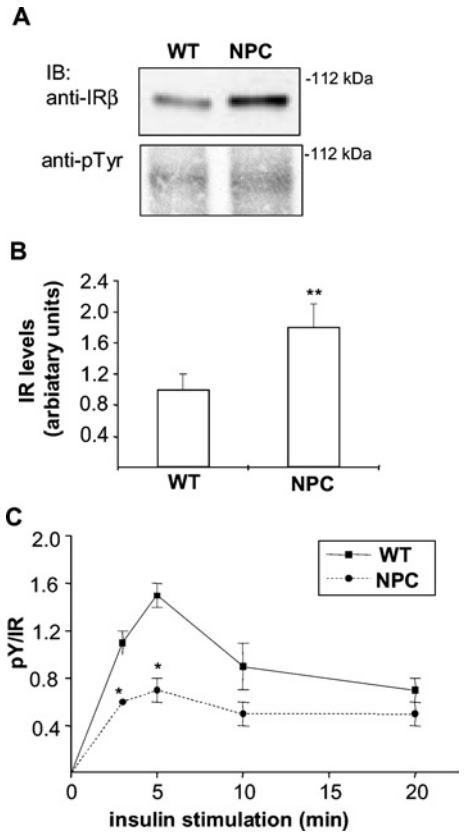

Figure 2 IR levels and activation in WT and NPC hepatocytes

(**A**) WT and NPC hepatocytes were stimulated with insulin for 0–20 min and cell lysates were analysed by Western blotting for IR levels (with anti-IRβ antibody) and phosphorylation (with anti-pTyr antibody). Representative immunoblots (IB) after 5 min of insulin stimulation are shown. (**B**) Quantification of IR levels and (**C**) IR activation as a function of time. Values are means $\pm$ S.E.M., $n = 44$ in (**B**) and $n = 4$–6 in (**C**). $^{*}P < 0.05$, $^{**}P < 0.001$, P values from a two-tailed Student's t test in all experiments.

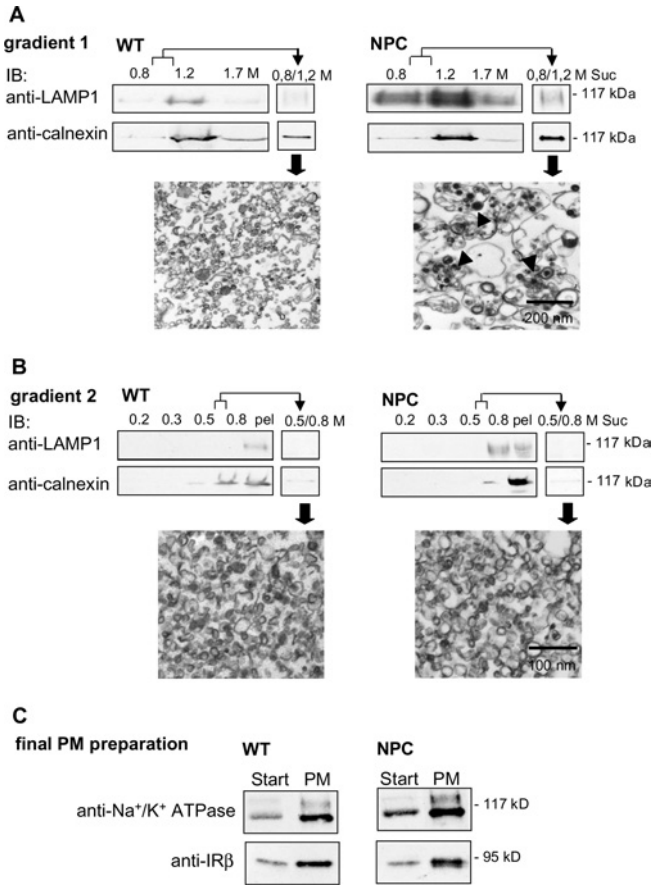

Figure 3 Isolation of PM fractions from WT and NPC mouse livers

Plasma membranes were isolated by sequential density-gradient centrifugation as detailed in the Experimental section. (**A**, **B**) Depletion of contaminating membranes in the preparation. The distribution of lysosomal and ER marker proteins LAMP1 and calnexin respectively in the gradient fractions and interphases was analysed by Western blotting. Interphases represent the membrane fractions collected from gradient 1 and subjected to gradient 2 (0.8/1.2 M) (**A**), and the final plasma-membrane fraction was collected from gradient 2 (0.5/0.8 M) (**B**). Electron micrographs of the interphases are also shown. Arrowheads indicate storage organelles. Suc, sucrose; pel, pellet. Equal volumes of the gradient fractions were used for Western-blot analysis. (**C**) Enrichment of plasma-membrane proteins in the preparation. Na^+/K^+-ATPase and IR were immunoblotted from the starting material ('Start'; crude liver lysate subjected to gradient 1) and from the final plasma-membrane fraction (PM). To be able to compare the band intensities in the same blot, 40 μg of protein was used for Start and 10 μg for plasma membrane.

the lysosomal marker LAMP1 and the ER marker calnexin were detected in both WT and NPC preparations. In electron micrographs of the fractions, storage organelles were observed in NPC samples (see 0.8/1.2 M sucrose interphase in Figure 3A). The membranes were subjected to a second gradient for further purification. After this gradient, the final plasma-membrane preparations in WT and NPC appeared to be morphologically similar, with approx. 20–50 nm diameter vesicular profiles, and only trace amounts of calnexin and no LAMP1 was detected (see 0.5/0.8 M sucrose interphase in Figure 3B). The contaminating membranes were mostly recovered in the pellet at the bottom of the gradient (Figure 3B). In the final preparation, the plasma-membrane proteins IR and Na^+/K^+-ATPase were found to be approx. 8-fold enriched in comparison with the starting material (Figure 3C; note that the amount of protein immunoblotted from the starting material was four times higher than that from plasma-membrane preparation).

IR activation in isolated plasma membranes

To study IR activation in the isolated membranes, we set up an *in vitro* assay for measuring IR activity. Under the assay conditions, IR activation was strictly dependent on the presence of insulin and ATP (Figure 4A). Similar to intact cells, the activation of IR in NPC plasma membranes was defective in comparison with WT membranes (Figure 4B). This result suggested that the cause of the impaired IR activation in NPC cells was indeed present in the plasma membrane. To investigate whether excess phosphatase activity accounts for the defect, we performed the IR activation assay in the isolated membranes in the presence of phosphatase inhibitors. The inhibitors caused a small increase in IR activation in both WT and NPC samples but the difference between the samples was maintained (results not shown), suggesting that increased phosphatase activity was not responsible for the compromised IR activation in NPC cells.

Plasma-membrane lipid composition and fluidity

To gain insight into the structure of the NPC liver plasma membranes, the lipid composition of the membranes was analysed by MS. The analysis revealed that the amount of cholesterol was approx. 2-fold higher in the NPC plasma membrane, as indicated by the elevated cholesterol/PL ratio (Figure 5A). A previous study reported a 10-fold excess of cholesterol in NPC mouse liver

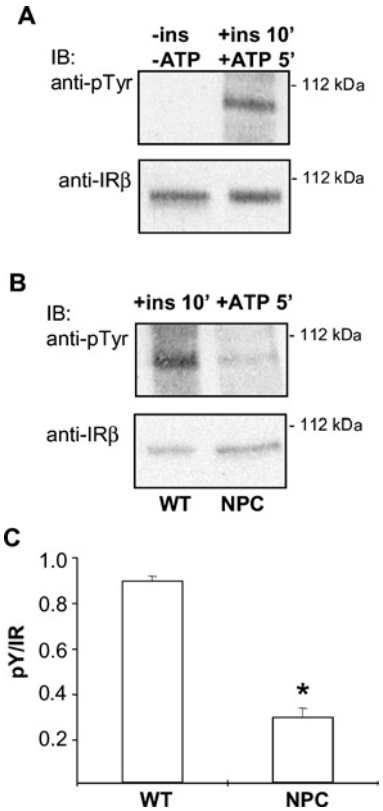

Figure 4 IR activation in isolated plasma membranes

(**A**) Validation of the IR *in vitro* kinase assay. Under the assay conditions, IR phosphorylation in the isolated membranes is strictly dependent on insulin and ATP. (**B**) Comparison of IR activation in WT and NPC plasma-membrane preparations. Representative immunoblots are shown. (**C**) Quantification of the data. Values are means ± S.E.M., $n = 6$, $^*P < 0.05$.

lysates [28], lending further support to the notion that the plasma-membrane purification method used eliminated the bulk of the late endosomal/lysosomal storage organelles. We also found that the acyl chain saturation of major PLs, SM and PC in particular, was increased in the NPC plasma membrane, and the fatty acyl chain lengths of these lipids were decreased (Figure 5B). Membrane fluidity was then determined on the basis of fluorescence polarization of DPH. We found that the DPH anisotropy values were significantly higher in NPC membranes as compared with WT (0.221 ± 0.002 in NPC versus 0.166 ± 0.001 in WT membranes, $P < 0.001$). Together, these data are consistent with a more ordered phase (i.e. lipid raft), favouring the structure of the NPC plasma membrane. Such a structure would be expected to affect the function and dynamics of lipid rafts and raft-associated proteins.

Analysis of DRMs

Association with low-density DRMs is a commonly used biochemical criterion to assess the raft association of molecules. We therefore studied the detergent resistance of IR and known raft and non-raft lipids. First, we analysed the detergent resistance of IR in the isolated plasma membranes. The membranes were lysed in the presence of 1 % Triton X-100 at 4 °C, subjected to Optiprep density gradient centrifugation, and the amount of IR in the different fractions was analysed by Western blotting as described in [13]. In the absence of insulin, IR is normally recovered in the detergent-soluble fractions [13], and such a distribution was seen in WT samples (Figure 6A). In NPC membranes, however, a small fraction of the receptor was recovered in DRMs (Figure 6A). To study the distribution of the ligand-occupied IR, we performed the experiment in intact hepatocytes using ^{125}I-labelled insulin as a marker for the active receptor. The cells were treated with the radiolabelled ligand for 5 min, washed extensively and fractionated as above. Unspecific binding (< 2 %

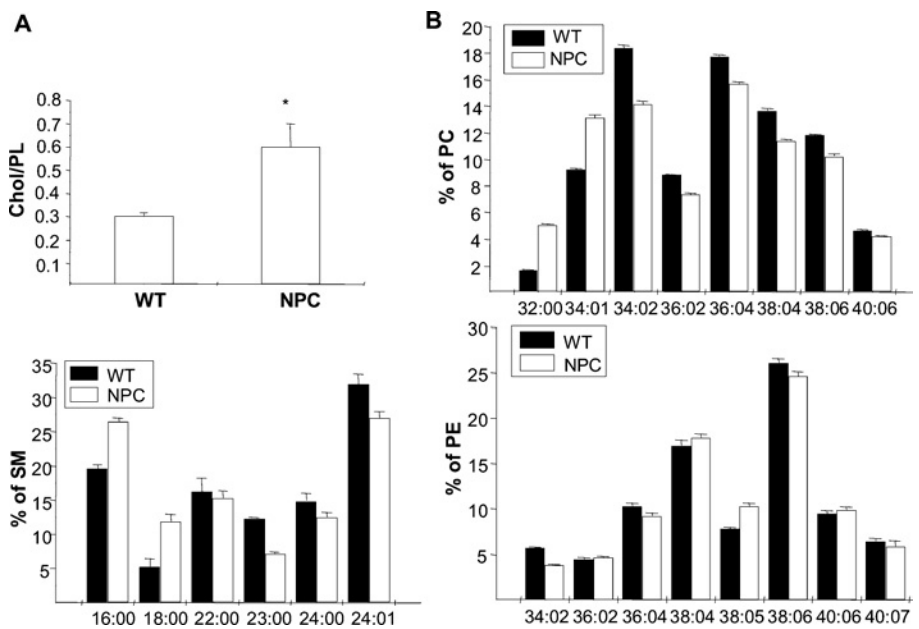

Figure 5 MS analysis of WT and NPC plasma-membrane lipid composition

(**A**) Cholesterol/PL ratio. Values are means ± S.D. for two independent determinations performed in triplicate. $^*P < 0.05$. The total amount of PLs was not significantly different between NPC and WT samples. (**B**) Acyl chain lengths and saturation of major PL classes. Species constituting a minimum of 5 % of total in each PL class are included. Values are means ± S.D. for a representative experiment performed in triplicate. PE, phosphatidyl ethanolamine.

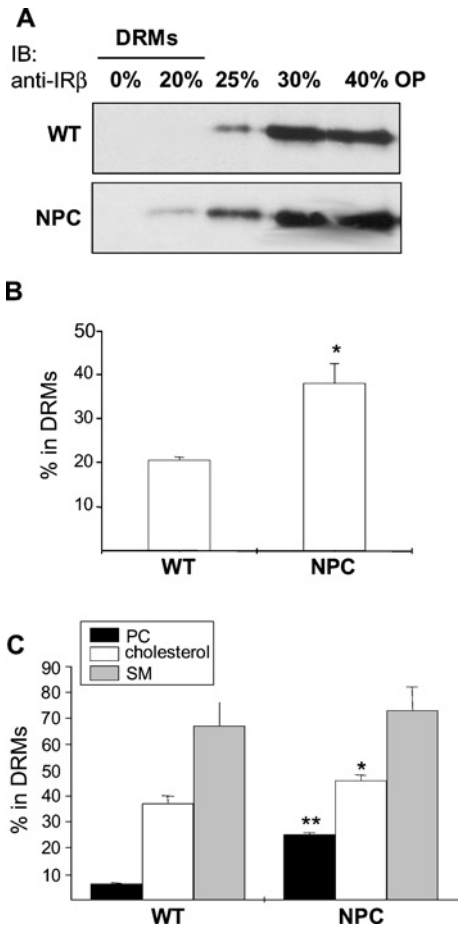

Figure 6 Association of IR, cholesterol, SM and PC with DRMs

(**A**) Isolated plasma membranes from WT and NPC mouse livers were solubilized in 1 % Triton X-100 at 4 °C and subjected to Optiprep density-gradient centrifugation. Proteins from the gradient fractions were precipitated with trichloroacetic acid and analysed by Western blotting with anti-IRβ antibodies. OP, Optiprep. (**B**) For analysing the fraction of ligand-occupied IR in DRMs, WT and NPC hepatocytes were stimulated with ^{125}I-insulin, washed and subjected to density-gradient centrifugation. The amount of radioactivity in the fractions was determined and the percentage in DRMs is indicated. (**C**) The fraction of radiolabelled lipids in DRMs from WT and NPC hepatocytes. Black bars, [^{3}H]PC; white bars, [^{14}C]cholesterol; grey bars, [^{3}H]SM. The cells were labelled and the lipids were analysed as detailed in the Experimental section. Values are means $\pm$ S.D. for three to four independent experiments performed in triplicate; $^*P < 0.05$, $^{**}P < 0.001$.

of the radioactivity in all experiments) was subtracted from the values. The DRMs from NPC cells contained approx. 50 % more label than the respective fractions from WT cells (Figure 6B). These findings suggest that the raft affinity of both the unbound and ligand-bound IR was increased in the NPC membranes as compared with control.

We also studied the DRM association of cholesterol, SM and PC in WT and NPC hepatocytes. Of these, PC is a major component of detergent-soluble membranes, whereas cholesterol and SM associate avidly with DRMs. The cells were labelled with [^{14}C]cholesterol or [^{3}H]choline for 24 h and subjected to gradient centrifugation. Before analysing the amounts of labelled lipids in the fractions, the [^{3}H]choline-labelled lipids PC and SM were separated by TLC. Interestingly, all of the lipids exhibited a tendency towards increased DRM association in NPC cells, although, in the case of SM, the difference was not statistically significant (Figure 6C). The most pronounced difference was seen in the DRM association of PC (6 % in WT cells versus

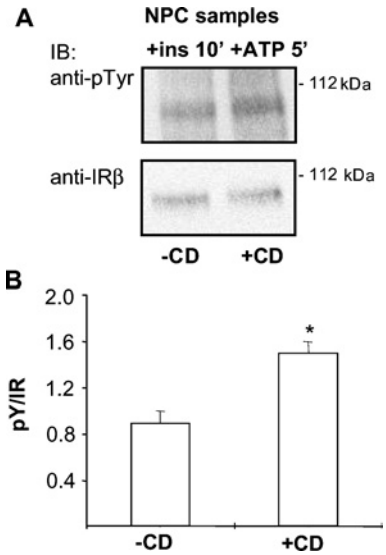

Figure 7 Effect of cholesterol removal on IR activation in isolated NPC plasma membranes

Isolated NPC plasma membranes were treated with methyl-β-cyclodextrin (CD; 10 mM for 30 min at 37 °C) and the IR activation assay was performed as in Figure 4. Representative immunoblots (**A**) with quantification of the data (**B**) are shown. Values in (**B**) are means $\pm$ S.E.M., $n = 10$, $^*P < 0.05$.

25 % in NPC cells). This probably reflects the changes in PC fatty acyl chain composition observed in NPC, and indicates that both raft- and non-raft-favouring lipids exhibit increased detergent resistance in NPC membranes.

Effect of cholesterol removal on IR activation

As our data showed that the amount of cholesterol and the association of IR with DRMs were increased in the NPC plasma membrane, we tested the effect of cholesterol removal on IR activation. Cholesterol extraction by methyl-β-cyclodextrin inhibits the association of the activate IR with DRMs and attenuates insulin signalling in normal hepatocytes [13]. However, in living cells, this treatment causes global changes in plasma-membrane architecture and function by e.g. affecting the actin cytoskeleton, and thus the observed effects may not be solely due to raft disruption [29]. We therefore used the plasma-membrane preparations to analyse the effect of methyl-β-cyclodextrin-mediated cholesterol depletion on IR activation. In WT membranes, a decrease in IR activity was observed, in accordance with previous reports [13,30] (results not shown). In NPC membranes, however, cholesterol removal significantly improved IR activation (Figures 7A and 7B). These findings suggest that an excess of cholesterol, or possibly, unfavourable partitioning of molecules between membrane domains due to the altered lipid composition, impairs insulin signalling in NPC hepatocytes, and that this defect can be restored by removing cholesterol from the membrane.

DISCUSSION

In the present study, we show up-regulation and defective functioning of a key signalling molecule, IR, in primary hepatocytes from the NPC mouse. We also report on altered composition, detergent resistance and fluidity of plasma-membrane lipids, which appear as the underlying cause for the IR dysfunction. This idea is strongly supported by the finding that changing the lipid environment rescues IR activation in the NPC plasma membrane.

Our results suggest that the amount of cholesterol in the NPC hepatocyte plasma membrane is increased. While a similar result was obtained in NPC fibroblasts [22], in some studies, the NPC plasma membrane was found to be cholesterol-depleted [31]. Yet, in other reports, no changes in the plasma-membrane cholesterol levels were observed [32–34]. The different methodologies used and materials analysed make comparisons between the studies difficult. To our knowledge, the present study represents the first assessment of the plasma-membrane lipid composition in NPC hepatocytes. Notably, hepatocytes are highly specialized cells in terms of cholesterol metabolism. For instance, they take up HDL (high-density lipoprotein) cholesterol via the scavenger receptor SR-B1 (reviewed in [35]). The mechanism of cholesterol uptake, and fate of the cholesterol internalized via this route, differs from that of LDL cholesterol. A major proportion of HDL-associated sterol associates with the plasma membrane with fast kinetics, apparently bypassing late endosomes and lysosomes [36,37]. This cholesterol flux affects the hepatocyte plasma-membrane lipid composition differently from several other cell types. Moreover, elevated plasma-membrane cholesterol levels are not necessarily incompatible with an endosomal cholesterol trafficking defect. Although the basic defect in cells lacking NPC1 is likely to be endo/lysosomal, the endosomal cholesterol transport block is leaky [38] and, at least in cells with massive lipid loading, the plasma membrane might eventually become cholesterol-engorged. In fact, considering the recently reported early endosomal cholesterol enrichment in NPC cells [39], one would have to postulate a cholesterol concentration gradient between the plasma membrane and early endosomes if the cell surface was cholesterol-depleted.

Another lipid compositional change observed in the NPC plasma-membrane preparations was an increased fatty acyl chain saturation of major PLs. This agrees with earlier findings in NPC fibroblasts [32]. Increases in the cholesterol content and fatty acyl chain saturation would both be predicted to decrease membrane fluidity. Two lines of evidence suggest that the NPC hepatocyte plasma membrane is indeed less fluid than the plasma membrane of control hepatocytes. First, the NPC membranes displayed increased DPH anisotropy values and, secondly, the most abundant plasma-membrane lipids were increasingly detergent-resistant. These parameters are interdependent, i.e. DRMs represent a more ordered subset of the plasma membrane [40]. Moreover, the increased DRM association of IR suggests that, in NPC hepatocytes, the receptor partitioned into a more ordered lipid environment than in control cells.

Methyl-β-cyclodextrin treatment of plasma-membrane vesicles is known to lead to commensurate decreases in lipid order [40]. This offers a likely explanation for the stimulatory effect of methyl-β-cyclodextrin on IR activation in the NPC plasma membrane. By removing cholesterol, methyl-β-cyclodextrin restores membrane fluidity and thereby alleviates IR activation. This finding not only agrees with the notion that the NPC plasma-membrane lipid composition favours increased lipid ordering but also provides further support to the idea that the lipid compositional changes observed are not due to contaminating endo/lysosomal membranes.

We have previously shown that, in normal hepatocytes, methyl-β-cyclodextrin-mediated cholesterol depletion impaired IR activation [13]. Thus it seems that there is a delicate balance in the degree of lipid ordering that optimally assists IR signalling – too little as well as too much ordering may be deleterious. The interdependence of membrane lipids and IR activity has been assessed in several studies. For instance, feeding of exogenous lipids, e.g. fatty acids or cholesterol derivatives, has been shown to alter the composition of cell membranes as well as IR activity [41,42]. Moreover, in aging Wistar rats that become insulin-resistant, increased plasma-membrane viscosity was found to associate with decreased IR activity [43]. In the light of the current data, these findings may well be compatible with the concept of raft-dependent IR signalling.

The present study represents the first report on insulin signalling in the NPC model. The observed up-regulation of the IR in NPC cells was a highly reproducible finding and conceivably compensates for poor receptor activation. Interestingly, increased IR expression is not restricted to murine NPC hepatocytes but is also found in the murine brain (S. Vainio and E. Ikonen, unpublished work) as well as in several NPC1 fibroblast lines in a genome-wide gene expression analysis (S. Pfeffer, personal communication). Although apparently compensated for by receptor levels in murine NPC hepatocytes, uncompensated defects of insulin signalling in NPC disease could be envisioned to have major effects on several cellular processes, such as energy metabolism and survival of neuronal cells.

The basis of the 'fatty liver' formation in NPC disease is considerably different from that in more common pathological conditions. The liver is the organ where most of the cholesterol and fatty acids, both from dietary sources and of endogenous origin, are processed. Moreover, hepatocytes have the tendency to accumulate lipid in response to various harmful stimuli, e.g. Western-type diet [44]. Hepatocyte lipid storage occurs mostly in the form of cytoplasmic lipid droplets composed of a neutral lipid (triacylglycerol and cholesteryl ester) core. However, recent data suggest that close connections between some pools of cholesterol in the plasma membrane and lipid droplets may exist, and point to the interdependence of cellular triacylglycerol and cholesterol compartmentalization [45,46]. We speculate also that more commonly observed fatty changes of the liver could perturb plasma-membrane lipid organization and thereby contribute to the development of hepatic insulin resistance [47].

We thank K. Lindros (National Public Health Institute, Helsinki, Finland) for sharing his knowledge and laboratory equipment, D. Tosh (Department of Biology and Biochemistry, University of Bath, Bath, U.K.) for indispensable help with setting up the hepatocyte isolation method, and A. Uro, T. Grunström and L. Arala for technical assistance. This study was financially supported by the Ara Parseghian Medical Research Foundation, the Academy of Finland, the Sigrid Juselius Foundation, the Finnish Medical Society Duodecim (grant to S.V.) and the Science Foundation of Helsinki University (Young Investigator's grant to S.V.).

REFERENCES

1 Ikonen, E. and Holtta-Vuori, M. (2004) Cellular pathology of Niemann-Pick type C disease. Semin. Cell Dev. Biol. **15**, 445–454
2 Ory, D. S. (2000) Niemann-Pick type C: a disorder of cellular cholesterol trafficking. Biochim. Biophys. Acta **1529**, 331–339
3 Patterson, M. C. and Pentchev, P. G. (1996) Niemann-Pick; type C. Neurology **46**, 1785–1786
4 Reid, P. C., Sugii, S. and Chang, T. Y. (2003) Trafficking defects in endogenously synthesized cholesterol in fibroblasts, macrophages, hepatocytes, and glial cells from Niemann-Pick type C1 mice. J. Lipid Res. **44**, 1010–1019
5 Simons, K. and Ikonen, E. (1997) Functional rafts in cell membranes. Nature (London) **387**, 569–572
6 Simons, K. and Toomre, D. (2000) Lipid rafts and signal transduction. Nat. Rev. Mol. Cell Biol. **1**, 31–39
7 Bickel, P. E. (2002) Lipid rafts and insulin signaling. Am. J. Physiol. Endocrinol. Metab. **282**, E1–E10
8 Saltiel, A. R. and Pessin, J. E. (2003) Insulin signaling in microdomains of the plasma membrane. Traffic **4**, 711–716
9 Saltiel, A. R. and Kahn, C. R. (2001) Insulin signalling and the regulation of glucose and lipid metabolism. Nature (London) **414**, 799–806
10 White, M. F. and Kahn, C. R. (1994) The insulin signaling system. J. Biol. Chem. **269**, 1–4

11 White, M. F. and Yenush, L. (1998) The IRS-signaling system: a network of docking proteins that mediate insulin and cytokine action. Curr. Top. Microbiol. Immunol. **228**, 179–208
12 Uhles, S., Moede, T., Leibiger, B., Berggren, P. O. and Leibiger, I. B. (2003) Isoform-specific insulin receptor signaling involves different plasma membrane domains. J. Cell Biol. **163**, 1327–1337
13 Vainio, S., Heino, S., Mansson, J. E., Fredman, P., Kuismanen, E., Vaarala, O. and Ikonen, E. (2002) Dynamic association of human insulin receptor with lipid rafts in cells lacking caveolae. EMBO Rep. **3**, 95–100
14 Loftus, S. K., Morris, J. A., Carstea, E. D., Gu, J. Z., Cummings, C., Brown, A., Ellison, J., Ohno, K., Rosenfeld, M. A., Tagle, D. A. et al. (1997) Murine model of Niemann-Pick C disease: mutation in a cholesterol homeostasis gene. Science **277**, 232–235
15 Liscum, L. (2000) Niemann-Pick type C mutations cause lipid traffic jam. Traffic **1**, 218–225
16 Simons, K. and Gruenberg, J. (2000) Jamming the endosomal system: lipid rafts and lysosomal storage diseases. Trends Cell Biol. **10**, 459–462
17 Voikar, V., Rauvala, H. and Ikonen, E. (2002) Cognitive deficit and development of motor impairment in a mouse model of Niemann-Pick type C disease. Behav. Brain Res. **132**, 1–10
18 Smets, F. N., Chen, Y., Wang, L. J. and Soriano, H. E. (2002) Loss of cell anchorage triggers apoptosis (anoikis) in primary mouse hepatocytes. Mol. Genet. Metab. **75**, 344–352
19 Tosh, D., Alberti, G. M. and Agius, L. (1988) Glucagon regulation of gluconeogenesis and ketogenesis in periportal and perivenous rat hepatocytes. Heterogeneity of hormone action and of the mitochondrial redox state. Biochem. J. **256**, 197–204
20 Nakabayashi, H., Taketa, K., Miyano, K., Yamane, T. and Sato, J. (1982) Growth of human hepatoma cells lines with differentiated functions in chemically defined medium. Cancer Res. **42**, 3858–3863
21 Heino, S., Lusa, S., Somerharju, P., Ehnholm, C., Olkkonen, V. M. and Ikonen, E. (2000) Dissecting the role of the Golgi complex and lipid rafts in biosynthetic transport of cholesterol to the cell surface. Proc. Natl. Acad. Sci. U.S.A. **97**, 8375–8380
22 Blom, T. S., Koivusalo, M., Kuismanen, E., Kostiainen, R., Somerharju, P. and Ikonen, E. (2001) Mass spectrometric analysis reveals an increase in plasma membrane polyunsaturated phospholipid species upon cellular cholesterol loading. Biochemistry **40**, 14635–14644
23 Folch, J., Lees, M. and Sloane Stanley, G. H. (1957) A simple method for the isolation and purification of total lipides from animal tissues. J. Biol. Chem. **226**, 497–509
24 Kawato, S., Kinosita, Jr, K. and Ikegami, A. (1977) Dynamic structure of lipid bilayers studied by nanosecond fluorescence techniques. Biochemistry **16**, 2319–2324
25 Holtta-Vuori, M., Tanhuanpaa, K., Mobius, W., Somerharju, P. and Ikonen, E. (2002) Modulation of cellular cholesterol transport and homeostasis by Rab11. Mol. Biol. Cell **13**, 3107–3122
26 Jarett, L., Schweitzer, J. B. and Smith, R. M. (1980) Insulin receptors: differences in structural organization on adipocyte and liver plasma membranes. Science **210**, 1127–1128
27 Zhang, M., Dwyer, N. K., Love, D. C., Cooney, A., Comly, M., Neufeld, E., Pentchev, P. G., Blanchette-Mackie, E. J. and Hanover, J. A. (2001) Cessation of rapid late endosomal tubulovesicular trafficking in Niemann-Pick type C1 disease. Proc. Natl. Acad. Sci. U.S.A. **98**, 4466–4471
28 Xie, C., Turley, S. D., Pentchev, P. G. and Dietschy, J. M. (1999) Cholesterol balance and metabolism in mice with loss of function of Niemann-Pick C protein. Am. J. Physiol. **276**, E336–E344
29 Kwik, J., Boyle, S., Fooksman, D., Margolis, L., Sheetz, M. P. and Edidin, M. (2003) Membrane cholesterol, lateral mobility and the phosphatidylinositol 4,5-bisphosphate-dependent organization of cell actin. Proc. Natl. Acad. Sci. U.S.A. **100**, 13964–13969
30 Gustavsson, J., Parpal, S., Karlsson, M., Ramsing, C., Thorn, H., Borg, M., Lindroth, M., Peterson, K. H., Magnusson, K. E. and Stralfors, P. (1999) Localization of the insulin receptor in caveolae of adipocyte plasma membrane. FASEB J. **13**, 1961–1971
31 Dahl, N. K., Reed, K. L., Daunais, M. A., Faust, J. R. and Liscum, L. (1992) Isolation and characterization of Chinese hamster ovary cells defective in the intracellular metabolism of low density lipoprotein-derived cholesterol. J. Biol. Chem. **267**, 4889–4896
32 Koike, T., Ishida, G., Taniguchi, M., Higaki, K., Ayaki, Y., Saito, M., Sakakihara, Y., Iwamori, M. and Ohno, K. (1998) Decreased membrane fluidity and unsaturated fatty acids in Niemann-Pick disease type C fibroblasts. Biochim. Biophys. Acta **1406**, 327–335
33 Lange, Y., Ye, J., Rigney, M. and Steck, T. (2000) Cholesterol movement in Niemann-Pick type C cells and in cells treated with amphiphiles. J. Biol. Chem. **275**, 17468–17475
34 Lange, Y., Ye, J., Rigney, M. and Steck, T. L. (2002) Dynamics of lysosomal cholesterol in Niemann-Pick type C and normal human fibroblasts. J. Lipid Res. **43**, 198–204
35 Silver, D. L. and Tall, A. R. (2001) The cellular biology of scavenger receptor class B type I. Curr. Opin. Lipidol. **12**, 497–504
36 Wustner, D. (2005) Mathematical analysis of hepatic high density lipoprotein transport based on quantitative imaging data. J. Biol. Chem. **280**, 6766–6779
37 Wustner, D., Mondal, M., Huang, A. and Maxfield, F. R. (2004) Different transport routes for high density lipoprotein and its associated free sterol in polarized hepatic cells. J. Lipid Res. **45**, 427–437
38 Lusa, S., Blom, T. S., Eskelinen, E. L., Kuismanen, E., Mansson, J. E., Simons, K. and Ikonen, E. (2001) Depletion of rafts in late endocytic membranes is controlled by NPC1-dependent recycling of cholesterol to the plasma membrane. J. Cell Sci. **114**, 1893–1900
39 Choudhury, A., Sharma, D. K., Marks, D. L. and Pagano, R. E. (2004) Elevated endosomal cholesterol levels in Niemann-Pick cells inhibit rab4 and perturb membrane recycling. Mol. Biol. Cell **15**, 4500–4511
40 Gidwani, A., Holowka, D. and Baird, B. (2001) Fluorescence anisotropy measurements of lipid order in plasma membranes and lipid rafts from RBL-2H3 mast cells. Biochemistry **40**, 12422–12429
41 Bruneau, C., Hubert, P., Waksman, A., Beck, J. P. and Staedel-Flaig, C. (1987) Modifications of cellular lipids induce insulin resistance in cultured hepatoma cells. Biochim. Biophys. Acta **928**, 297–304
42 Meuillet, E. J., Leray, V., Hubert, P., Leray, C. and Cremel, G. (1999) Incorporation of exogenous lipids modulates insulin signaling in the hepatoma cell line, HepG2. Biochim. Biophys. Acta **1454**, 38–48
43 Nadiv, O., Shinitzky, M., Manu, H., Hecht, D., Roberts, Jr, C. T., LeRoith, D. and Zick, Y. (1994) Elevated protein tyrosine phosphatase activity and increased membrane viscosity are associated with impaired activation of the insulin receptor kinase in old rats. Biochem. J. **298**, 443–450
44 Mach, T. (2000) Fatty liver – current look at the old disease. Med. Sci. Monit. **6**, 209–216
45 Le Lay, S., Krief, S., Farnier, C., Lefrere, I., Le Liepvre, X., Bazin, R., Ferre, P. and Dugail, I. (2001) Cholesterol, a cell size-dependent signal that regulates glucose metabolism and gene expression in adipocytes. J. Biol. Chem. **276**, 16904–16910
46 Pol, A., Martin, S., Fernandez, M. A., Ferguson, C., Carozzi, A., Luetterforst, R., Enrich, C. and Parton, R. G. (2004) Dynamic and regulated association of caveolin with lipid bodies: modulation of lipid body motility and function by a dominant negative mutant. Mol. Biol. Cell **15**, 99–110
47 Ikonen, E. and Vainio, S. (2005) Lipid microdomains and insulin resistance: is there a connection? Science STKE 2005, pe3

Received 18 March 2005/2 June 2005; accepted 9 June 2005
Published as BJ Immediate Publication 9 June 2005, doi:10.1042/BJ20050460